Design of a Lanthanum Bromide Detector for Time-of-Flight PET

A. Kuhn, S. Surti, *Member, IEEE*, J. S. Karp, *Senior Member, IEEE*, P. S. Raby, K. S. Shah, A. E. Perkins, *Member, IEEE*, and G. Muehllehner, *Fellow, IEEE*

***Abstract*—Recent improvements in the growth and packaging of lanthanum bromide ($LaBr_3$), in addition to its superb intrinsic properties of high light output, excellent energy resolution, and fast decay time, make it a viable detection material for a positron emission tomography (PET) scanner based on time-of-flight (TOF). We have utilized theoretical simulations and experimental measurements to investigate the design and performance of pixelated $LaBr_3$ Anger-logic detectors suitable for use in a TOF PET scanner. Our results indicate that excellent energy resolution can be obtained from individual as well as multicrystal arrays of $LaBr_3$ in a 4 mm $\times$ 4 mm $\times$ 30 mm geometry. Measured energy resolutions (at 511 keV) of 4.1% for a single crystal and an average of 5.1% for an array of 100 crystals have been achieved with our best samples. Both simulations and experimental measurements of an Anger-logic based detector consisting of the $LaBr_3$ crystal array coupled to a continuous light guide and seven photomultiplier tubes (PMTs), have resulted in the ability to clearly discriminate 511 keV interactions in each crystal. We have measured coincidence time resolutions for both 0.5% and 5.0% cerium-doped $LaBr_3$ and found that the higher level of Ce-doping yielded superior results with little to no degradation in light output or energy resolution. The time resolution for a single 5.0% Ce-doped $LaBr_3$ crystal (4 mm $\times$ 4 mm $\times$ 30 mm) coupled directly to a PMT was measured to be 275 ps full-width at half-maximum (FWHM). With an array of 100 crystals coupled to a light guide and seven PMT cluster an average time resolution of 290 ps FWHM was obtained by summing the signals from the PMT cluster. Ultimately, two 5.0% Ce-doped $LaBr_3$ Anger-logic detectors placed in coincidence yielded a time resolution of 313 ps FWHM.**

***Index Terms*—Anger-logic, gamma-ray detectors, lanthanum detectors, positron emission tomography, scintillation detectors, 3-D PET, time resolution, time-of-flight.**

I. Introduction

THE incorporation of time-of-flight (TOF) has long been recognized for its potential to improve positron emission tomography (PET) scanner performance [1]–[3]. One of the major challenges in TOF PET is finding an ideal scintillator. In recent years, there has been resurgence in the search for an ideal scintillator (i.e., one having high light output, high stopping power, fast decay time, and good linearity) [4]–[6]. Out of the considerable research and development of inorganic scintillators [7]–[12], the possibility for TOF PET has recently been proposed for both LSO [13] and lanthanum scintillators [14].

Of particular interest to us is the lanthanum bromide ($LaBr_3$) scintillator. The high light output ($\sim$61 000 photons per MeV), fast decay time ($\sim$35 ns), and excellent energy resolution (2.8% at 662 keV) of $LaBr_3$ [11] make it a viable detection material for a PET scanner based on TOF. The high light output allows the use of long narrow crystals (i.e., 4 mm $\times$ 4 mm $\times$ 30 mm), thus maintaining high sensitivity and spatial resolution in a scanner. Excellent energy resolution allows for improved rejection of scattered events and reduction in random coincidences, which are limiting factors of image quality in three-dimensional (3-D) PET. The fast decay and excellent coincidence time resolution will reduce dead time as well as random coincidences. Here, we will evaluate the design and performance of a pixelated $LaBr_3$ detector suitable for use in a whole-body 3-D PET scanner incorporating TOF.

II. Detector Design

The proposed $LaBr_3$ detector design is based on previous designs of pixelated GSO and NaI(Tl) detectors used in 3-D PET [15], [16]. The detector consists of an array of individual 4 mm $\times$ 4 mm $\times$ 30 mm $LaBr_3$ crystals (hermetically sealed and packed in a reflective powder) coupled to a continuous light guide and array of photomultiplier tubes (PMTs). Fig. 1 illustrates the arrangement of the pixelated Anger-logic detector.

The scintillation light from the crystals is distributed to multiple PMTs, via the light guide, to allow the photon interaction position and energy to be determined. In this arrangement, the PMTs are packed in a hexagonal array and the light guide thickness is chosen such that the light spread from a crystal positioned directly above the PMT center is limited to a cluster of seven PMTs. The crystal dimensions are chosen to maintain good spatial resolution and detection efficiency in a potential 3-D PET scanner. A singles detection efficiency of $\sim$51% is obtained with 30 mm thick $LaBr_3$ ($\mu = 0.47$ cm^{-1}) for events with energies above 400 keV.

III. Measurements With Single $LaBr_3$ Crystals

Several single crystal samples of $LaBr_3$ were evaluated in order to characterize energy resolution, coincidence time resolution and light output in a 4 mm $\times$ 4 mm $\times$ 30 mm geometry

Manuscript received November 14, 2003; revised February 13, 2004. This work was supported in part by the U.S. Department of Energy under Grant DE-FG02-88ER60642, in part by the National Institutes of Health under Grants R21EB001684 and 1R43-EB00477-01, and in part by a research agreement with Saint-Gobain Crystals and Detectors.

A. Kuhn, S. Surti, and J. S. Karp are with the University of Pennsylvania, Philadelphia, PA 19104 USA (e-mail: akuhn@rad.upenn.edu; surti@rad.upenn.edu; karp@rad.upenn.edu).

P. S. Raby is with Saint-Gobain Crystals and Detectors, Newbury, OH 44065 USA (e-mail: Paul.S.Raby@saint-gobain.com).

K. S. Shah is with Radiation Monitoring Devices, Watertown, MA 02472 USA (e-mail: kshah@rmdinc.com).

A. E. Perkins and G. Muehllehner are with Philips Medical Systems, Philadelphia, PA 19104 USA (e-mail: amy.perkins@philips.com; gerd.muehllehner@philips.com).

Digital Object Identifier 10.1109/TNS.2004.835777

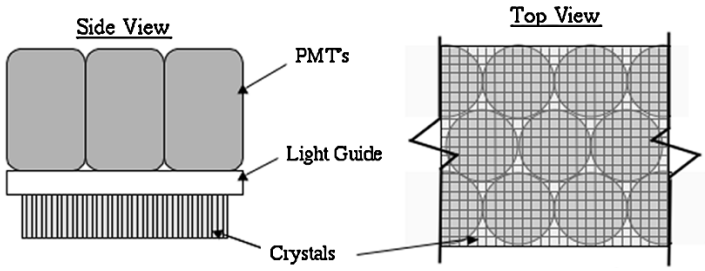

Fig. 1. Two views of a pixelated Anger-logic detector illustrating the arrangement of the PMTs, light guide, and scintillator crystals. Note the hexagonal PMT arrangement in the top view.

as well as differences in varying cerium concentration. $LaBr_3$ samples (each encapsulated and packed in reflective powder) were obtained from Radiation Monitoring Devices, Inc. (RMD) and Saint-Gobain Crystals and Detectors (Saint-Gobain). Three small $LaBr_3$ samples with Ce concentrations of 0.5%, 5.0%, and 10% were obtained from RMD with varying geometries (each less than $\sim$1 cm^3 in volume). The two samples obtained from Saint-Gobain were each polished and in a 4 mm $\times$ 4 mm $\times$ 30 mm geometry with Ce concentrations of 0.5% and 5.0%.

Each of the Saint-Gobain samples were tested with the 4 mm $\times$ 4 mm cross section optically coupled to the center of the PMT photocathode. Fig. 2(a) and (b) show measured pulse shapes obtained by digitizing the PMT anode output for 511 keV energy deposition in four $LaBr_3$ samples and one LYSO sample included for comparison.

The pulse shapes indicate that both rise and decay times improve (i.e., reduce) with increasing Ce concentration while the total light output measured for the 0.5% and 5.0% Saint-Gobain crystals remains the same. Additionally, the measured light output for the 4 mm $\times$ 4 mm $\times$ 30 mm $LaBr_3$ crystals was approximately twice that of a 4 mm $\times$ 6 mm $\times$ 25 mm LYSO crystal, with the 5.0% Ce crystal having faster rise and decay times. The improvement is more significant from 0.5% to 5.0% Ce [see Fig. 2(b)] than 5.0% to 10.0% Ce [see Fig. 2(a)]. Our simulations indicate that the difference in sample geometry largely accounts for the 1/3 reduction in light output between the small ($<$1 cm^3) samples and 4 mm $\times$ 4 mm $\times$ 30 mm samples (see Table I).

The energy resolution of each sample was measured with the crystals optically coupled to the center of the PMT photocathode and excited by 511 keV photons from a ^{68}Ge source. The signals from the PMT anode were input directly into a charge integrating analog-to-digital converter (ADC) with an integration time of 120 ns. Fig. 3 shows the energy spectrum generated for the Saint-Gobain 5.0% Ce $LaBr_3$ sample. The energy spectrum was calibrated by exciting the crystal with 662 keV photons from a ^{137}Cs source.

Additionally, the coincidence time resolution for each $LaBr_3$ sample was measured. This measurement was accomplished by irradiating a BC-418 plastic scintillator (coupled to a XP2020Q PMT) and each $LaBr_3$ sample coupled to a 50 mm diameter XP20Y0 PMT (a fast, eight-stage version of the XP2020Q without a quartz window) with 511 keV positron annihilation photon pairs from a ^{68}Ge source. The signal from the plastic-PMT detector was processed by an Ortec 934 CFD

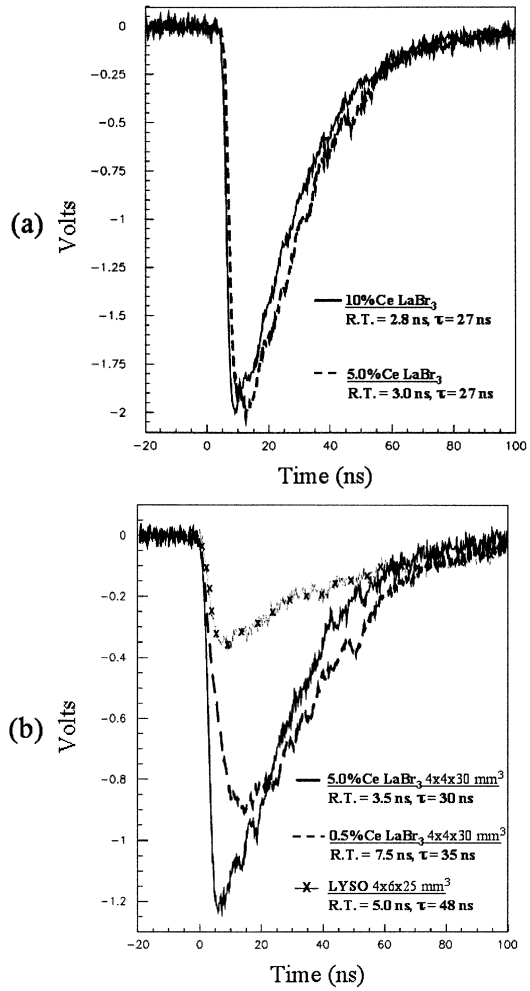

Fig. 2. Single pulse shapes measured at 511 keV for (a) two RMD $LaBr_3$ samples (10% and 5.0% Ce, each $\sim$1 cm^3 in volume) and (b) two Saint-Gobain samples (5.0% and 0.5% Ce, each 4 mm $\times$ 4 mm $\times$ 30 mm) and one LYSO sample of similar geometry for comparison. The 10–90 rise time (RT) and decay time (τ) are given for each pulse. The pulse shapes were measured with the crystals directly coupled to a Photonis XP2020Q PMT (tube rise time $\sim$1.5 ns).

and formed the "start" channel of the timing circuit. The $LaBr_3$-PMT detector was processed by a LeCroy 825 Z rise time–compensated discriminator and delay forming the "stop" channel. The time difference was digitized with a time-to-digital converter (TDC) having 45 ps per bin resolution. Fig. 4 shows the coincidence timing resolution spectrum obtained for the Saint-Gobain 5.0% Ce $LaBr_3$ crystal.

TABLE I
RESULTS WITH SINGLE $LaBr_3$ SAMPLES

$LaBr_3$ Manufacturer (size)	%Ce	ΔE/E (at 511 keV)	Time Resolution (FWHM)	Rise Time	Decay Time	Relative Light Output
RMD Inc. (<1 cm³)	0.5	3.5%	----	7.0 ns	33 ns	1.50
RMD Inc. (<1 cm³)	5.0	3.7%	250 ps	3.0 ns	27 ns	1.56
RMD Inc. (<1 cm³)	10.0	4.7%	245 ps	2.8 ns	27 ns	1.46
Saint-Gobain (4x4x30 mm³)	0.5	4.1%	350 ps	7.5 ns	35 ns	1.00
Saint-Gobain (4x4x30 mm³)	5.0	4.5%	275 ps	3.5 ns	30 ns	1.00

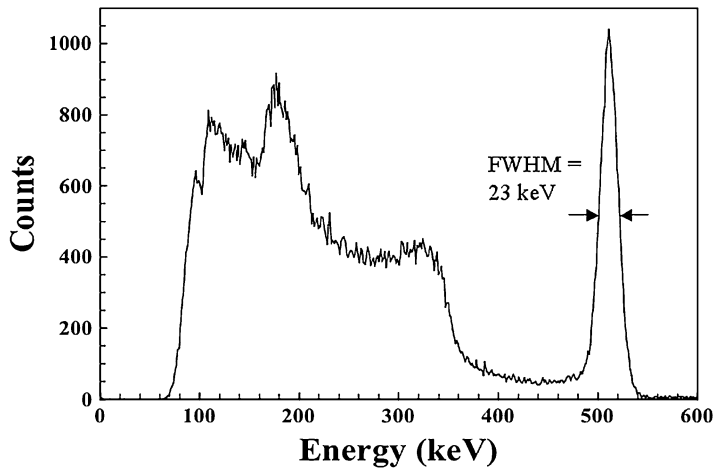

Fig. 3. Energy spectrum measured at 511 keV with the Saint-Gobain 5.0% Ce $LaBr_3$ (4 mm × 4 mm × 30 mm) crystal optically coupled to the center of the PMT photocathode. For this pixel, an energy resolution of 23 keV FWHM ($\Delta E/E = 4.5\%$) was obtained by fitting the photopeak with a Gaussian distribution.

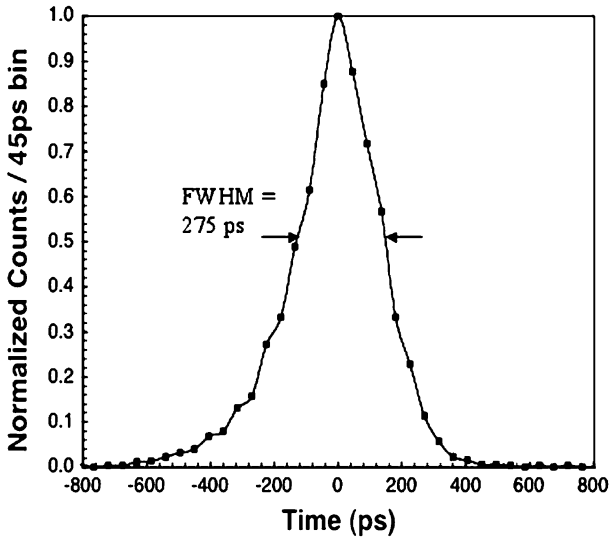

Fig. 4. Timing resolution spectrum measured with the Saint-Gobain 5.0% Ce $LaBr_3$ (4 mm × 4 mm × 30 mm) crystal optically coupled to the center of a XP20Y0 PMT photocathode in coincidence with a BC-418 plastic scintillator coupled to a XP2020Q. A time resolution of 275 ps FWHM was obtained. A time resolution of 235 ps FWHM was measured for two BC-418 plastic scintillators in coincidence.

Results from the energy and time resolution measurements for each of the samples are shown in Table I (values for energy resolution ±0.2% and time resolution ±5 ps). Additionally, the rise and decay time as well as the samples relative light output (normalized to the Saint-Gobain 0.5% Ce sample) are listed in the table. Excellent energy resolution is measured for both small RMD samples and the full size Saint-Gobain crystals. In general, samples with higher Ce concentration (having faster rise and decay times with approximately equal light output) had better time resolution with a greater improvement between the 0.5% and 5.0% Ce (4 mm × 4 mm × 30 mm) samples as compared the 5.0% and 10.0% Ce samples. The time resolution measured for the 5.0% Ce sample from RMD is consistent with previous measurements reported by Shah *et al.* [17]. Degradation in time resolution from 250 ps to 275 ps FWHM is measured between the small 5.0% Ce RMD sample and the 5.0% Ce Saint-Gobain sample. This degradation is consistent with findings based on different sample geometries in other fast scintillators [13], [18].

IV. MEASUREMENTS WITH A $LaBr_3$ ANGER-LOGIC DETECTOR

A. Methods

We have received several multicrystal (10 × 10 and 5 × 5) arrays of 0.5% and 5.0% Ce $LaBr_3$ from Saint-Gobain. Each array consisted of individually cut and polished 4 mm × 4 mm × 30 mm crystals (with 0.3 mm spacing) optically coupled to a 3 mm glass window, packed in a reflective powder and hermetically sealed in an aluminum housing.

In order to test energy resolution, timing resolution, and relative light output of each crystal in the array as well as the ability to discriminate 511 keV events in each crystal with a 7 PMT Anger-logic detector, a data acquisition system utilizing both a TDC and ADC was implemented. Fig. 5 illustrates a block diagram layout of the acquisition system.

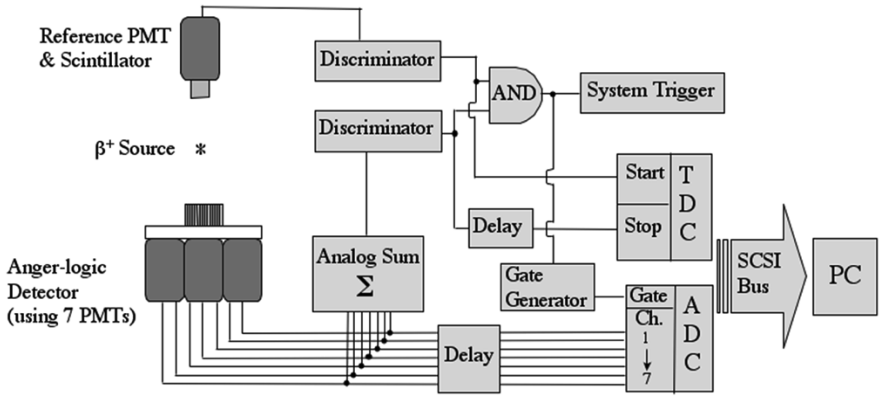

Fig. 5. Block diagram showing the electronics architecture used to acquire data. A coarse coincidence gate of 30 ns (set in the AND logic unit) is used as the system trigger. Following a triggered event, the amount of charge integrated in each ADC channel and the time difference recorded by the TDC are processed via PC software. Processing included correction of ADC offsets and PMT gains, implementation of a weighted centroid algorithm to determine the interaction location, and position and energy gating to generate time and energy spectra for individual crystals.

Each crystal array was tested in an Anger-logic arrangement consisting of the $LaBr_3$ crystal array optically coupled to a 1.6 cm thick light guide (UVT Lucite) and cluster of seven PMTs (hexagonally arranged). While both 39 mm and 50 mm PMTs were considered in the detector design, the measurements presented hereafter represent the results obtained with a 7 PMT cluster of 50 mm diameter Photonis XP20Y0 PMTs. It was found that these PMTs provided coincidence time resolution performance close to that of the XP2020Q at a much reduced cost.

B. Results

Two-dimensional flood maps of photon interaction positions in the crystal array were generated by implementing a weighted centroid algorithm on the ADC data obtained from each of the seven PMTs following events from a 511 keV source. For crystal identification purposes this was done without requiring the coincidence with the reference detector shown in Fig. 5. Fig. 6(a) shows the two-dimensional (2-D) flood map for events having a total energy >450 keV in a 5.0% Ce $LaBr_3$ array with 100 crystals. Fig. 6(b) shows a histogram for a center row of crystals in the 2-D flood. The crystal discrimination for this array was typical of all the crystal arrays received.

Coincidence time resolution measurements with the Anger-logic detector were made in a similar fashion to those described in Section III (i.e., with the plastic-PMT detector forming the "start" and $LaBr_3$ detector forming the "stop"). Here, however, the seven PMT signals were summed before being processed by the discriminator (see Fig. 5). We found that summing the seven PMT signals before processing in the discriminator yielded better time resolution than processing a single PMT with the largest pulse (i.e., the central PMT). This is illustrated in Fig. 7, showing the time resolution measured with a single 5.0% Ce $LaBr_3$ (4 mm × 4 mm × 30 mm) crystal in three different arrangements. In position 1 [shown for reference, see Fig. 7(a)] the crystal is directly coupled to the PMT and a time resolution of 275 ps FWHM is measured (as reported in Section III). With the crystal coupled to a light guide and positioned above the center of a seven PMT cluster [position 2, Fig. 7(a)] the time resolution degrades to 350 ps FWHM when using only the signal from the central PMT in the timing circuit. The degradation is largely due to the fact that only a fraction of the total light out of the crystal is processed by any single PMT in the cluster (i.e., about 70% of the total light is incident upon the central PMT with the crystal in position 2). However, the time resolution is improved to 300 ps FWHM when all seven PMT signals are summed. This improvement is more dramatic (465 ps to 310 ps) when the crystal is positioned above the edge of the central PMT (position 3). The difference in time resolution measured for the crystal coupled directly to the PMT and in the Anger-logic arrangement (275 ps compared to 300 ps) is primarily due to light loss in the Anger-logic arrangement (i.e., coupling interfaces, gaps between PMTs, etc.) and differences in PMT responses (i.e., transit times, transit time spreads, etc.). While it is recognized that the coincidence time resolution may be improved by correcting for PMT transit time differences, the measurements presented here do not incorporate a correction.

In order to obtain coincidence time resolution for crystals in the arrays, position, and energy gates were implemented in software prior to generating a histogram of time differences between the reference detector (plastic-XP2020Q) and the $LaBr_3$ Anger-logic detector. The location of the position gate for each crystal was determined from the 2-D flood map [see Fig. 6(a)]. Additionally, an energy gate was placed on the events in a crystal such that the total energy deposited in the crystal was > 450 keV. Fig. 8 shows the coincidence time resolution measured for crystals in the 0.5% and 5.0% Ce $LaBr_3$ arrays as a function of crystal position (in the X- and Y-direction) in the Anger-logic detector. Consistent time resolution results are obtained for both crystal arrays with a ∼170 ps improvement measured for the 5.0% Ce array. An average coincidence time resolution of 308±18 ps is measured for all the crystals in the 5.0% Ce array with little variation in resolution over the center region of the seven PMT cluster. The average time resolution for crystals in each of the arrays is given in Table II.

The energy resolution and relative light output were measured for each crystal in the arrays by similarly applying position gating. Excellent energy resolution was obtained for crystals in 0.5% and 5.0% Ce arrays with little degradation from the measurements with single crystals coupled directly to a PMT.

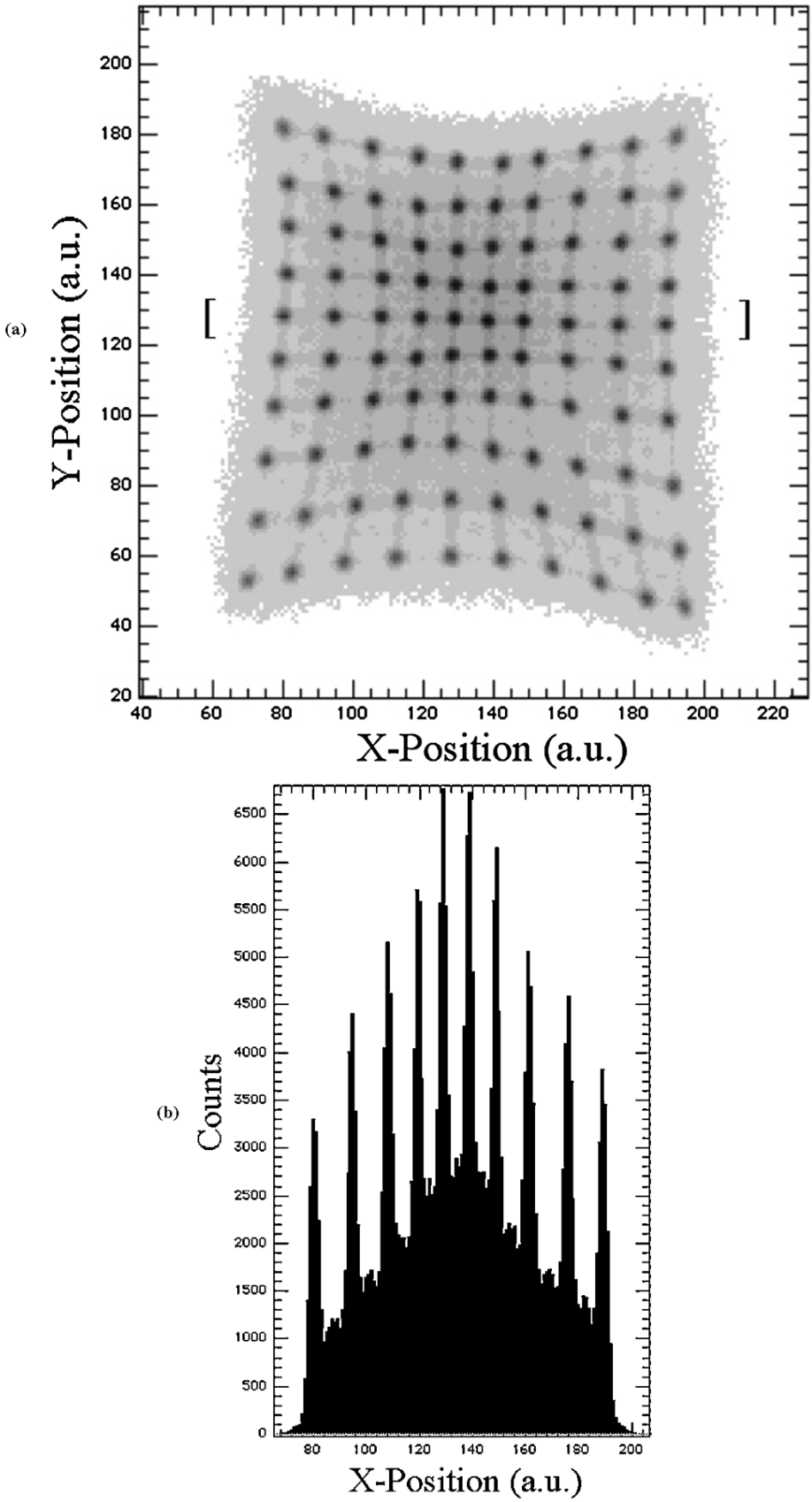

Fig. 6. (a) 2-D flood map of interaction positions for events >450 keV in a 5.0% Ce $LaBr_3$ array with 100 crystals coupled to a 1.6 cm light guide and cluster of 7 XP20Y0 PMTs. (b) Histogram of events for the fifth row of crystals from the top summed over 4 mm in the Y-direction [see brackets in (a)]. Note that the shape of the distribution in (b) (i.e., increased counts in the center of the distribution) is due to the geometric efficiency of the crystal array when irradiated by a point source at $\sim$30 cm distance.

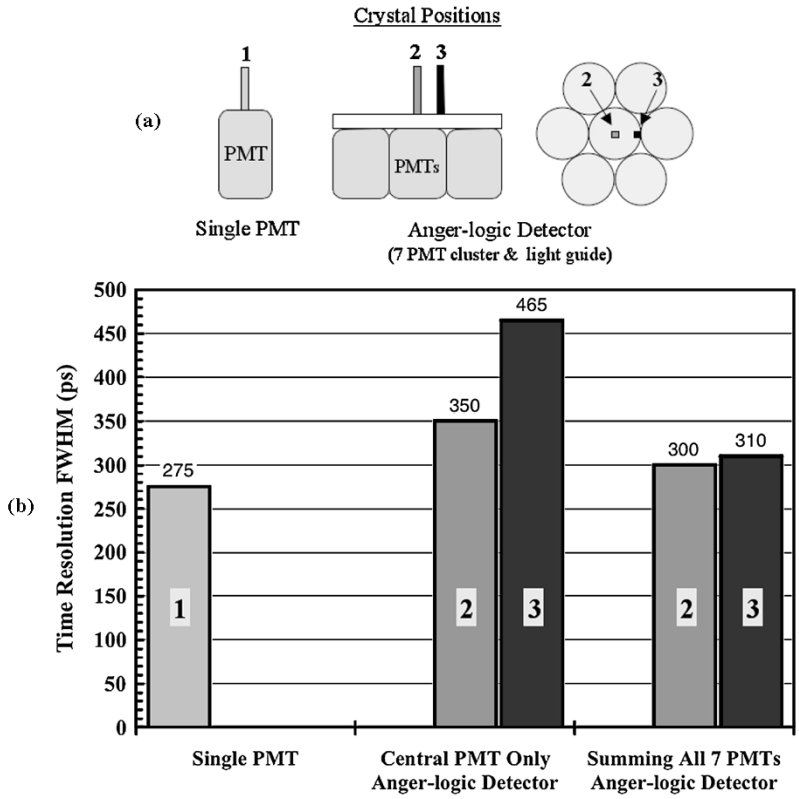

Fig. 7. (a) PMT and crystal arrangement for the three measured positions. In the Anger-logic arrangement both side and top views of the detector are shown. (b) Coincidence time resolution for a single 5.0% Ce $LaBr_3$ (4 mm × 4 mm × 30 mm) crystal coupled to a single PMT (labeled 1) and array of PMTs using the central and sum of seven PMTs (for crystal positions 2 and 3). Note the improvement for both position 2 and 3 with all 7 PMT's summed.

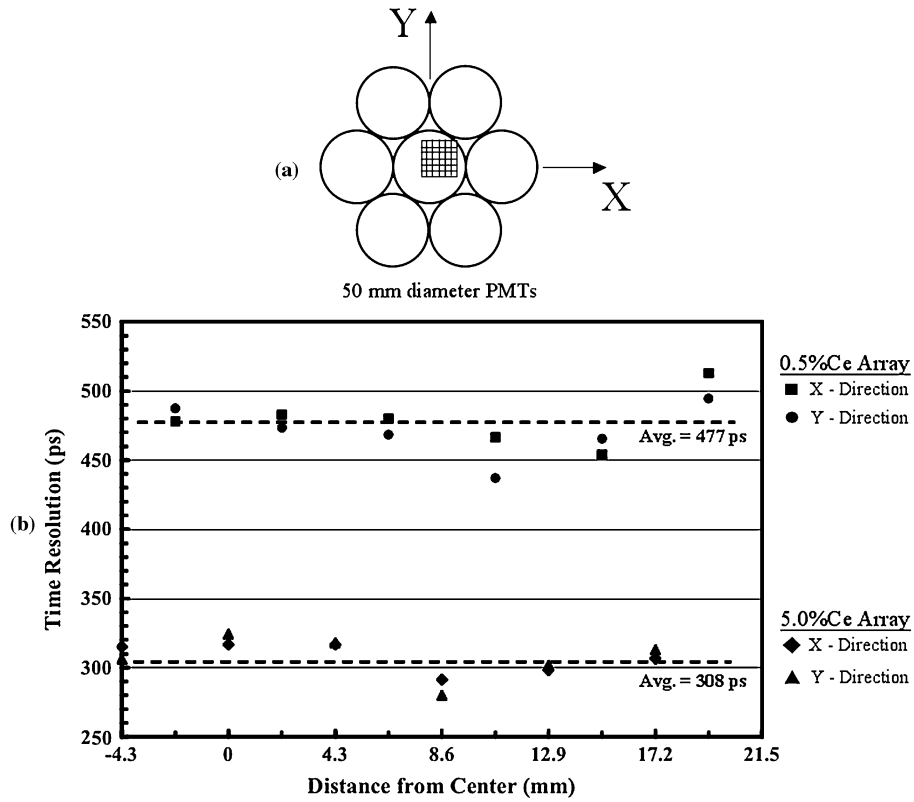

Fig. 8. (a) Arrangement of the seven PMT cluster and crystal array relative to the X- and Y-coordinate axis. (b) Coincidence time resolution for crystals in the 0.5% and 5.0% Ce arrays at various positions above the seven PMT cluster. Each point represents the average time resolution for two crystals at locations along each coordinate direction. The dashed lines indicate the average time resolution for the crystals in each array.

TABLE II
RESULTS WITH $LaBr_3$ CRYSTAL ARRAYS

Array	% Ce	# Crystals	Average ΔE/E at 511 keV	Relative Light Output	σ_{LO}	Average Time Resolution (FWHM)
1	0.5	100	5.31% ± 0.44%	1.25	3%	477 ± 23 ps
2	0.5	100	5.41% ± 0.45%	1.19	3%	481 ± 29 ps
3	0.5	100	5.20% ± 0.40%	1.29	2%	469 ± 20 ps
4	0.5	100	5.47% ± 0.45%	1.37	2%	455 ± 19 ps
5	5.0	25	5.65% ± 0.59%	1.31	4%	308 ± 18 ps
6	5.0	25	5.42% ± 0.42%	1.30	6%	300 ± 13 ps
7	5.0	100	5.08% ± 0.68%	1.37	3%	290 ± 10 ps

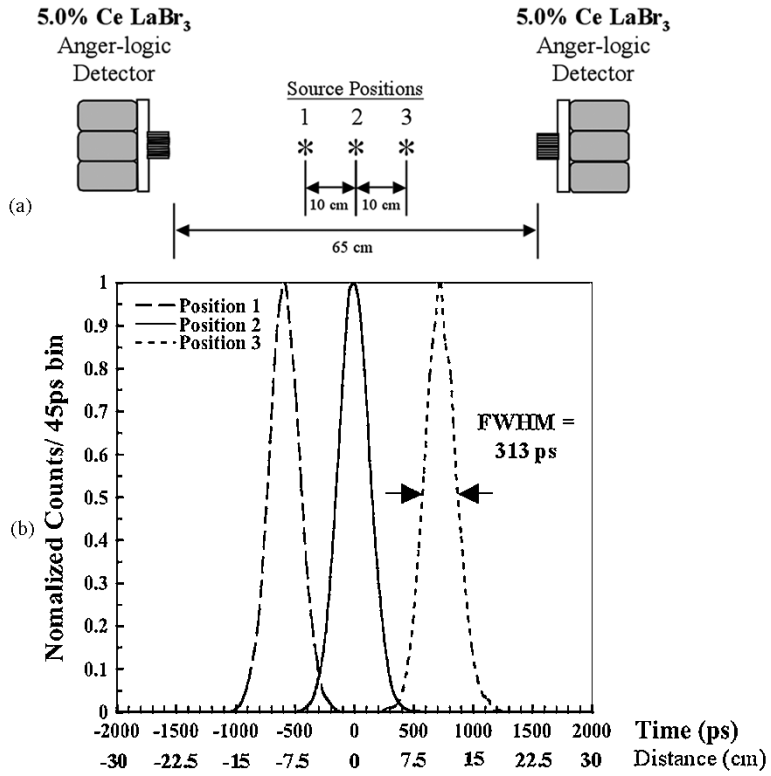

Fig. 9. (a) Arrangement of the two Anger-logic detectors and the three source positions. (b) Three measured time spectra for the source positions in (a). A time resolution of approximately 313 ps FWHM was obtained for each of the spectra. Note that the time scale is also given in units of distance and thus the time peaks correspond to an uncertainty in position of about 4.7 cm FWHM.

An average $\Delta E/E \sim 5.4\%$ was obtained for crystals in the arrays (see Table II) with little variation between crystals. The relative light output in Table II represents the average for the crystals in the array and is given relative to the single 4 mm × 4 mm × 30 mm samples tested in Section III. Light output equal to or better than the single crystal samples is obtained with little variation (i.e., low standard deviation in light output, σ_{LO}), thus indicating crystals in the arrays are well polished and packed in reflective powder.

V. COINCIDENCE TIME RESOLUTION FOR TWO $LaBr_3$ ANGER-LOGIC DETECTORS

The time resolution for two $LaBr_3$ Anger-logic detectors (array numbers 5 and 6, see Table II) placed in coincidence was measured similarly to the timing measurements described in Section IV; however, the reference plastic-PMT detector was replaced with a second $LaBr_3$ Anger-logic detector. Each detector consisted of the $LaBr_3$ crystal array coupled to a light guide and cluster of seven PMTs (each a 50 mm diameter XP20Y0). The electronics shown in Fig. 5 for a single $LaBr_3$ detector was duplicated for the second detector allowing the interaction position and energy to be determined in the crystal arrays of both detectors.

Position and energy gates were placed on individual crystals in each detector allowing coincidence time spectra to be generated for pairs of crystals (i.e., events which deposit >450 keV in a single crystal in each detector). The two detectors were separated by 65 cm and irradiated with positron annihilation photon

pairs from a ^{68}Ge source. Fig. 9(a) illustrates the arrangement of the two Anger-logic detectors (each consisting of a 25 crystal 5.0% Ce $LaBr_3$ array) and the three source positions separated by 10 cm for which time spectra were measured. The coincidence time spectra measured at each source position for one pair of crystals are shown in Fig. 9(b).

A time resolution of 313 ps FWHM is obtained for each of the three spectra. This corresponds to an uncertainty in position $\Delta x = 4.7$ cm (obtained by using $\Delta x = c * \Delta t/2$, where c is the speed of light and Δt is the time resolution). Incorporating this time resolution into a TOF PET scanner is expected to significantly improve image signal-to-noise ratio and noise equivalent count-rate (NEC) [3], [14]. A similar measurement was performed with two 0.5% Ce $LaBr_3$ crystal arrays and a time resolution of 605 ps FWHM was measured. Additionally, a measurement with two LYSO crystal arrays yielded a time resolution of 640 ps FWHM.

VI. Conclusion

Our results show that excellent energy and time resolution is obtained with $LaBr_3$ crystals in a 4 mm $\times$ 4 mm $\times$ 30 mm geometry suitable for use in a whole body 3-D PET scanner. Samples with higher Ce concentration had faster rise and decay times (with approximately equal light output) and subsequently yielded superior coincidence time resolution. However, the improvement from 0.5% Ce to 5.0% Ce was more significant than the improvement from 5.0% Ce to 10.0% Ce.

Excellent crystal discrimination was achieved with Anger-logic detectors consisting of multicrystal arrays of 4 mm $\times$ 4 mm $\times$ 30 mm $LaBr_3$ coupled to a light guide and cluster of seven PMTs. The crystals in the arrays exhibited uniformity in light output and energy resolution. By summing the seven PMT signals, excellent time resolution is maintained over the central region of the cluster. A time resolution of 313 ps FWHM was obtained for two 5.0% Ce $LaBr_3$ Anger-logic detectors in coincidence.

By expanding the basic detector design to a pixelated $LaBr_3$ Anger-logic detector with a continuous light guide and hexagonal arrangement of PMTs, our results indicate excellent performance can be attained. As we have shown with previous NaI(Tl) and GSO detector designs, a dynamically chosen local cluster of seven PMTs can be utilized to determine the energy and position for each event. Using this method we have also achieved excellent and uniform time resolution.

Acknowledgment

The authors would like to thank W. Kononenko from the Physics Department, University of Pennsylvania, for providing electronic equipment used in data acquisition, C. Fontaine and P. Lavoute from Photonis for providing them with several PMTs for testing, and the research members at RMD Inc., Saint-Gobain, and Philips Medical Systems.

References

[1] R. Allemand, C. Gresset, and J. Vacher, "Potential advantages of a Cesium Flouride scintillator for time-of-flight positron camera," *J. Nucl. Med.*, vol. 21, pp. 153–155, 1980.

[2] N. A. Mullani, D. C. Ficke, R. Hartz, J. Markham, and G. Wong, "System design of a fast PET scanner utilizing time-of-flight," *IEEE Trans. Nucl. Sci.*, vol. NS-28, pp. 104–107, 1981.

[3] T. F. Budinger, "Time-of-flight positron emission tomography: Status relative to conventional PET," *J. Nucl. Med.*, vol. 24, pp. 73–78, 1983.

[4] C. W. E. van Eijk, "Inorganic scintillators in medical imaging," *Phys. Med. Biol.*, vol. 47, pp. R85–R106, 2002.

[5] S. E. Derenzo, M. J. Weber, E. Bourret-Courchesne, and M. K. Klintenberg, "The quest for the ideal inorganic scintillator," *Nucl. Instrum. Meth. A*, vol. 505, pp. 111–117, 2003.

[6] W. W. Moses, "Current trends in scintillator detectors and materials," *Nucl. Instrum. Meth. A*, vol. 487, pp. 123–128, 2002.

[7] A. Lempicki and J. Glodo, "Ce-doped scintillators: LSO and LuAP," *Nucl. Instrum. Meth. A*, vol. 416, pp. 333–344, 1998.

[8] K. S. Shah, J. Glodo, M. Klugerman, L. Cirignano, W. W. Moses, S. E. Derenzo, and M. J. Weber, "$LaCl_3$:Ce scintillator for γ-ray detection," *Nucl. Instrum. Meth. A*, vol. 505, pp. 76–81, 2003.

[9] E. van Loef, P. Dorenbos, C. W. E. van Eijk, K. W. Kramer, and H. U. Gudel, "High-energy-resolution scintillator: Ce^{3+} activated $LaCl_3$," *Appl. Phys. Lett.*, vol. 77, pp. 1467–1468, 2000.

[10] ——, "Scintillation properties of $LaBr_3$:Ce^{3+} crystals: Fast, efficient, and high-energy-resolution scintillators," *Nucl. Instrum. Meth. A*, vol. 486, pp. 254–258, 2002.

[11] ——, "High-energy-resolution scintillator: Ce^{3+} activated $LaBr_3$," *Appl. Phys. Lett.*, vol. 79, pp. 1573–1575, 2001.

[12] C. W. E. van Eijk, "New inorganic scintillators—Aspects of energy resolution," *Nucl. Instrum. Meth. A*, vol. 471, pp. 244–248, 2001.

[13] W. W. Moses and S. E. Derenzo, "Prospects for time-of-flight PET using LSO scintillator," *IEEE Trans. Nucl. Sci.*, vol. 46, pp. 474–478, 1999.

[14] S. Surti, J. S. Karp, G. Muehllehner, and P. S. Raby, "Investigation of Lanthanum scintillators for 3-D PET," *IEEE Trans. Nucl. Sci.*, vol. 50, pp. 348–354, 2003.

[15] S. Surti, J. S. Karp, R. Freifelder, and F. Liu, "Optimizing the performance of a PET detector using discrete GSO crystals on a continuous light guide," *IEEE Trans. Nucl. Sci.*, vol. 47, pp. 1030–1036, 2000.

[16] S. Surti, J. S. Karp, and G. Muehllehner, "Evaluation of Pixelated NaI(Tl) detectors for PET," *IEEE Trans. Nucl. Sci.*, vol. 50, pp. 24–31, 2003.

[17] K. S. Shah, J. Glodo, M. Klugerman, W. W. Moses, S. E. Derenzo, and M. J. Weber, "$LaBr_3$:Ce scintillators for gamma ray spectroscopy," *IEEE Trans. Nucl. Sci.*, vol. 50, pp. 2410–2413, 2003.

[18] S. I. Ziegler, H. Ostertag, W. K. Kuebler, W. J. Lorenz, and E. W. Otten, "Effects of scintillation light collection on the time resolution of a time-of-flight detector for annihilation quanta," *IEEE Trans. Nucl. Sci.*, vol. 37, pp. 574–579, 1990.